Molecular Biology of the Cell
Vol. 5, 1325–1339, December 1994

# Analysis of Transport and Targeting of Syndecan-1: Effect of Cytoplasmic Tail Deletions

**Heini M. Miettinen,*†‡ Susan N. Edwards,* and Markku Jalkanen***

*Centre for Biotechnology, FIN-20521 Turku, Finland; and †Department of Medical Biochemistry, University of Turku, FIN-20520 Turku, Finland

Submitted October 6, 1994; Accepted October 26, 1994
Monitoring Editor: Richard Hynes

Madin-Darby canine kidney (MDCK) cells and Chinese hamster ovary (CHO) cells were transfected with wild-type and cytoplasmic deletion mutants of mouse syndecan-1 to study the requirements for transport and polarized expression of this proteoglycan. Expression in MDCK cells revealed that wild-type syndecan-1 is directed to the basolateral surface via a brefeldin A-insensitive route. A deletion of the last 12 amino acids of the syndecan-1 cytoplasmic tail (CT22) was sufficient to result in the appearance of mutant proteoglycans at both the basolateral and apical cell surfaces. Treatment with brefeldin A was able to prevent apical transport of the mutants. We thus propose that the C-terminal part of the cytoplasmic tail is required for steady-state basolateral distribution of syndecan-1. In CHO cells a deletion of the last 25 or 33 amino acids of the 34-residue cytoplasmic domain (CT9 and CT1, respectively) resulted in partial retention of the mutants in the endoplasmic reticulum (ER). A deletion mutant lacking the last 12 amino acids (CT22) was not retained. Interestingly, the unglycosylated core proteins of the CT9 and CT1 mutants showed a significantly lower apparent molecular weight when analyzed by sodium dodecyl sulfate (SDS) polyacrylamide gel electrophoresis than wild-type syndecan-1. However, when CHO transfectants expressing the CT1 mutant were incubated with brefeldin A, causing fusion of the ER and Golgi, CT1 ran with an almost equally high apparent molecular weight as the wild-type molecule. This would suggest that syndecan-1 undergoes extensive post-translational modifications or forms an SDS-resistant dimer/complex after transit from the ER.

## INTRODUCTION

Heparin sulfate-bearing molecules at the cell surface are thought to act as coreceptors for both heparin-binding growth factors and extracellular matrix (ECM) proteins, thus participating in the regulation of cell behavior (for review see Rapraeger, 1993; Elenius and Jalkanen, 1994). In vivo these functions may well be mediated by the syndecans, a major family of transmembrane, and cell surface proteoglycans, which have been shown to bind a number of ECM molecules (Koda *et al.*, 1985; Saunders and Bernfield, 1988; Sun *et al.*, 1989; Salmivirta *et al.*, 1991) and to function as coreceptors for the binding of growth factors to tyrosine kinase receptors (Kiefer *et al.*, 1990; Rapraeger *et al.*, 1991; Yayon *et al.*, 1991).

To date, four members of the syndecan family (syndecan-1, -2, -3, and -4) have been identified and named after the initial and best characterized member, syndecan-1. The extracellular domains show the greatest divergence between members and, with the exception of the sites of potential glycosaminolglycan-attachment, are poorly conserved between species. In contrast, the transmembrane and cytoplasmic domains of the syndecans are extremely conserved (Figure 1A) (for review see Bernfield *et al.*, 1992; Jalkanen *et al.*, 1993). In particular, the cytoplasmic tail of syndecan-1 is identical across the species so far examined, unlike its extracellular domain. This conservation suggests first that the cytoplasmic domain of syndecan-1 is crucial for its function, and second that it has a conserved role across the syndecan family. To investigate the role of this do-

‡ Corresponding author and present address: Department of Microbiology, Montana State University, Bozeman, MT 59717.

main, we have constructed a series of cytoplasmic deletion mutants for murine syndecan-1 (Figure 1A) based on the regions of greatest conservation between the syndecans.

It has previously been proposed that the cytoplasmic tail of syndecan-1 binds to the intracellular cytoskeleton and may thus act as an anchor between the extracellular matrix and cytoskeleton (Rapraeger *et al.*, 1986). This suggestion was based on results from Triton X-100 (TX-100) extractions and coimmunofluorescence analysis. Our recent data, generated with these cytoplasmic deletion mutants, however, suggest that the insolubility of syndecan-1 in TX-100 is not caused by its cytoplasmic tail but rather by an interaction of the glycosaminoglycan chains with detergent insoluble molecules (Miettinen and Jalkanen, 1994).

In adult tissues syndecan-1 is principally expressed in epithelia, where it is localized to the basolateral surface. During development, however, high levels of syndecan-1 expression have also been demonstrated in mesenchymal tissues. The polarized distribution observed for syndecan-1 at the cell surface, both in culture (Rapraeger *et al.*, 1986) and in tissues (Hayashi *et al.*, 1987), implies that the cytoplasmic domain of syndecan-1 may contain targeting signals.

To examine whether precise requirements for the targeting and processing of syndecan-1 can account for the extreme conservation of the cytoplasmic tail of syndecan-1, we have expressed wild-type and three cytoplasmic deletion mutants in Madin-Darby canine kidney (MDCK) epithelial cells and Chinese hamster ovary (CHO) fibroblasts.

MDCK cells were used as a model system to investigate targeting of syndecan-1 in polarized cells. In polarized cells newly synthesized proteins are either 1) delivered directly to their final destination (e.g., MDCK cells), 2) transported first to the basolateral domain from which apical proteins are transcytosed to the apical side (e.g., hepatocytes), or 3) transported to the target domains by both routes (e.g., CaCo-2 intestinal cells) (for review see Mostov *et al.*, 1992; Matter and Mellman, 1994). In this paper we have shown that a deletion of the last 12 amino acids from the 34-residue cytoplasmic tail of syndecan-1 resulted in increased mistargeting of the molecule to the apical domain. This altered polarization was not due to changes in shedding or ECM binding.

Previous studies have shown that partial or complete deletions of the cytoplasmic tail of some viral and endogenous eukaryotic proteins resulted in slower transport of the proteins from the ER to the Golgi (for examples see Rose and Bergman, 1983; Wills *et al.*, 1984; Zuniga and Hood, 1986). Using the CHO fibroblast cell line, we examined whether deletion mutations in the cytoplasmic tail affect the transport and subcellular location of syndecan-1. Our results suggest that a deletion of the last 25 residues causes a partial retention of syndecan-1 in the ER and thus reduces normal processing of syndecan-1 in the Golgi.

We have also examined the effect of brefeldin A (BFA) on trafficking of syndecan-1. BFA is a fungal metabolite that has frequently been used as a tool to examine protein and membrane trafficking between different cellular compartments. In many cells BFA-treatment causes the Golgi to disperse and fuse with the endoplasmic reticulum (ER), resulting in accumulation of newly synthesized proteins in the ER (Misumi *et al.*, 1986; Doms *et al.*, 1989; Lippincott-Schwartz *et al.*, 1989). In MDCK cells, however, the Golgi stacks remain morphologically intact during BFA exposure (Hunziker *et al.*, 1991; Sandvig *et al.*, 1991; Apodaca *et al.*, 1993), whereas the trans-Golgi network forms tubular extensions that may fuse with the endosomes (Hunziker *et al.*, 1991; Lippincott-Schwartz *et al.*, 1991; Wagner *et al.*, 1994). BFA inhibits some apical and some basolateral sorting routes in MDCK cells (Low *et al.*, 1992; Apodaca *et al.*, 1993) and also influences basolateral to apical transcytosis (Hunziker *et al.*, 1991; Prydz *et al.*, 1992; Matter *et al.*, 1993; Barosso and Sztul, 1994). Our experiments indicated that BFA-treatment of MDCK cells had no effect on basolateral targeting of wild-type syndecan-1. In contrast, BFA treatment of MDCK transfectants expressing mutant syndecan-1 prevented the mistargeting to the apical surface and restored the wild-type basolateral localization. In CHO cells BFA led to fusion of the ER and Golgi, thus reversing some effects of the ER retention of the CT9 and CT1 mutants.

## MATERIALS AND METHODS

### *Expression Vectors and Transfections*

For stable expression in MDCK cells, inserts coding for wild-type or mutant mouse syndecan-1 were subcloned into the *Eco*RI site of pBGS, a vector containing an SR$\alpha$ promoter (Takebe *et al.*, 1988) and a neomycin-resistance cassette (a gift from Bruce Granger, Montana State University, Bozeman, MT). The constructs were transfected into the cells using commercial lipofectin (GIBCO/BRL, Grand Island, NY) (Felgner *et al.*, 1987) or transfectace according to Rose *et al.* (1991). Transfectants were selected with 0.5 mg/ml Geneticin (G418, Sigma, St. Louis, MO). Single colonies were isolated using cloning cylinders and tested for expression by immunofluorescence.

For stable expression in CHO cells, cDNAs encoding wild-type or mutant mouse syndecan-1 were subcloned into the *Eco*RI site of the amplifiable expression vector pFRSV (Simonsen and Levinson, 1983; Horwich *et al.*, 1985; Miettinen *et al.*, 1989). Transfections were performed as above, and stably expressing cells were selected by growth in 0.2 $\mu$M methotrexate. The vector was amplified with increasing concentrations of methotrexate (final concentration 20 $\mu$M).

### *Oligonucleotide-directed Mutagenesis*

cDNAs encoding mouse syndecan-1 mutants lacking parts of the cytoplasmic tail were created by oligonucleotide-directed mutagenesis using standard techniques (Zoller and Smith, 1982; Kunkel *et al.*, 1987). The construction of the tailless syndecan-1 (CT1) has been described elsewhere (Miettinen and Jalkanen, 1994). To generate a mutant containing nine amino acids in the cytoplasmic tail (CT9), the 22-base oligonucleotide 5′-A GGC AGC **TAA** GCT TTG GAG GAG-3′ was used, encoding a stop codon (bold letters) and a *Hin*dIII-site (AAGCTT)

to simplify detection of the mutant. The CT22 mutant lacking 12 amino acids out of the 34 amino acid cytoplasmic tail was constructed using the 23-mer 5'-GC GGT GCC **TAG** TTT AAA CCC ACC-3', containing a stop codon (bold letters) and a *Dra* I-restriction site (TTTAAA). The mutations were confirmed by restriction enzyme cleavage and dideoxy sequencing (Sanger *et al.*, 1977).

## Cell Culture

Transfected MDCK cells (strain II) were maintained in selection medium containing 0.5 mg/ml Geneticin in Dulbecco's modified Eagle's medium (DMEM) supplemented with 5% fetal bovine serum (FBS), 50 U/ml penicillin, and 50 mg/ml streptomycin.

Transfected CHO cells were maintained in $\alpha$-modified Eagle's medium containing 5% FBS, 50 U/ml penicillin, 50 mg/ml streptomycin, 20 $\mu$M methotrexate, and 4 $\mu$g/ml folic acid.

Fourteen to eighteen hours before each experiment increased expression was induced by adding 5 mM sodium butyrate into the medium (Gorman *et al.*, 1983).

Untransfected MDCK and CHO cells were cultured as described above, but without Geneticin, methotrexate, or sodium butyrate.

## Immunofluorescence Microscopy

To visualize cell surface syndecan-1, monolayers grown on glass coverslips were incubated for 1 h on ice with 50 $\mu$g/ml 281-2, a rat monoclonal antibody (mAb) against the ectodomain of mouse syndecan-1 (Jalkanen *et al.*, 1985). After washing cells were fixed with 2.5% paraformaldehyde (PFA) in phosphate-buffered saline (PBS) and then incubated for 1 h at room temperature (RT) with fluorescein isothyocyanate (FITC)-conjugated rabbit anti-rat IgG (Dako, Santa Barbara, CA). After extensive washing cells were mounted using Glycergel (Dako) containing 2.5 mg/ml 1,4-diazabicyclo-[2.2.2] octane to prevent bleaching.

To visualize cell surface and intracellular syndecan-1, cells were first fixed with 2.5% PFA and permeabilized with 0.5% TX-100 in PBS. Unspecific binding was blocked by incubation with 0.2% gelatin-PBS. Monolayers were incubated with 50 $\mu$g/ml 281-2 for 1 h at RT after extensive washing with FITC-rabbit anti-rat IgG. Whenever indicated in the figure legends, the cells were incubated for 5 h with 6 $\mu$g/ml BFA before fixation or chase. Mounting was carried out as above.

Staining of E-cadherin (uvomorulin) was carried out after fixation and permeabilization using a rat mAb against murine E-cadherin (uvomorulin) (DECMA, Sigma) and FITC-rabbit anti-rat IgG.

## Metabolic Labeling, TX-100 Extractions, and Immunoprecipitations

Cells were labeled overnight in sulfate-free DMEM containing 10% FBS and 0.125 mCi/ml $Na_2{}^{35}SO_4$ (carrier free). The cells were extracted 10 min on ice with an extraction buffer (EB) containing 10 mM tris (hydroxymethyl) aminomethane, 50 mM Na-acetate, 150 mM NaCl, 1% TX-100, and 1 mM phenylmethylsulfonyl fluoride at pH 7.5 (Rapraeger *et al.*, 1986). Tissue culture plates were scraped with a rubber policeman, insoluble material was pelleted by centrifugation, and the pellet was resuspended as previously described (Miettinen *et al.*, 1992). All fractions were precleared by incubation with Sepharose CL-4B followed by immunoprecipitation with 281-2 conjugated to Sepharose CL-4B. Samples were run on a 3–15% linear gradient sodium dodecyl sulfate-polyacrylamide gel electrophoresis (SDS-PAGE); gels were treated with 2,5-diphenyloxazole, dried, and exposed to Kodak (Rochester, NY) XAR-5 film at −70°C.

When the shedding of syndecan-1 was examined, the MDCK transfectants were grown to confluency on Transwell polycarbonate filters (3 $\mu$m pore, Costar, Cambridge, MA). Cells were labeled for 7 h with $Na_2{}^{35}SO_4$, the medium from the apical and basal side of the filter was transferred into Eppendorf tubes, the cells were extracted with EB at pH 7.5, and all fractions were immunoprecipitated. When the effect of BFA on transport and targeting was examined, the cells were labeled in the presence or absence of 10 $\mu$g/ml BFA.

To obtain more accurate quantitation of syndecan-1, samples were run on a 0.7% agarose gel containing 0.1% SDS (Heinegård *et al.*, 1985; Thornton *et al.*, 1986). Quantitations were carried out using a microcomputer image analysis system (Imaging Research, St. Catharine's, Ontario, Canada). Special care was taken to scan films that were not overexposed.

## Western Blotting

Cells grown on 5-cm dishes were incubated for 5 h at 37°C in the presence or absence of 6 $\mu$g/ml BFA before a 10-min extraction on ice with EB pH 7.5. After cell scraping the detergent-insoluble material was pelleted by centrifugation, and the detergent-soluble fraction was precipitated with 70% ethanol and pelleted in microfuge. Pellets were resuspended in sample buffer, heated to 95°C for 5 min, and separated by a linear 4–15% gradient SDS-polyacrylamide gel. The proteins were transferred onto a Hybond $N^+$ nylon membrane (Amersham, Arlington Heights, IL). The membrane was blocked for 30 min at RT with 10% nonfat dry milk in PBS, followed by 30 min at RT with 10% nonfat dry milk and 0.4% Tween-20 in PBS. All subsequent incubations and washes were carried out at RT in 0.4% Tween-20/PBS. The primary antibody, mouse syndecan-1 (281-2), was used at a concentration of 2.5 $\mu$g/ml, followed by horseradish peroxidase (HRP)-conjugated sheep anti-rat IgG (1:5000; Amersham). After extensive washing the membrane was incubated with enhanced chemiluminescence (ECL) Western blotting detection reagents according to the manufacturer's instructions (Amersham) and exposed to Kodak XAR-5 film for 0.5–5 min.

## Quantitation of Syndecan-1 Expression Levels

CHO or MDCK cells were released from tissue culture plates by gentle scraping of monolayers incubated in PBS + 1 mM EDTA on ice for 10 min. Cells were spun down and washed in PBS. Triplicate aliquots of the cell suspension were collected and used to determine cell number by incubation with crystal violet. Cell aliquots were mixed with 0.5% crystal violet in 20% ethanol and centrifuged at 10 000 × *g* for 10 min. The stained cell pellet was washed extensively with distilled water and resuspended in 10% acetic acid; the absorbance at 595 nm was measured. This method provided consistent results within the triplicates that agreed well with measurements obtained with a Coulter counter. The cells were collected from suspension by centrifugation and lysed in EB pH 7.5. After 15 min on ice, insoluble material was removed by centrifugation. Samples were normalized for cell numbers and blotted onto Hybond N+ membrane (Amersham) using a vacuum manifold. Syndecan-1 was then detected as described above for Western blots and quantified using a microcomputer image analysis system. The results obtained by this method were confirmed by Northern analysis.

## Analysis of Syndecan-1 Binding to ECM Proteins

MDCK cells were released from tissue culture plates as described above, and washed with PBS. Syndecan-1 was released from the cell surface by incubation with 25 $\mu$g/ml trypsin in PBS for 10 min on ice, followed by addition of Soybean trypsin inhibitor to a final concentration of 100 $\mu$g/ml. The cells were then removed by centrifugation, and the relative amounts of syndecan-1 present in the samples were determined as described above. Increasing amounts of collagen (Vitrogen-100, 95–98% type I, remainder type III, Celtrix, Santa Clara, CA) and fibronectin (human plasma) were blotted onto nitrocellulose (Schleicher and Schuell, Keene, NH) using a vacuum manifold. The filters were then incubated with 10% nonfat dry milk in PBS for 30 min and with 10% nonfat dry milk and 0.4% Tween-20 in PBS for 2 h at RT. The filters were then washed in PBS and incubated overnight at 4°C with wild-type and mutant syndecan-1 at equal concentrations

in PBS. After washing in PBS, bound syndecan-1 was immunodetected and quantified as described above.

### *Quantitation of Syndecan-1 Localization at the Apical and Basolateral Plasma Membranes Using [$^{125}$I]-Anti-Syndecan-1 Antibody 281-2*

MDCK cells were grown to confluency on Transwell polycarbonate filters. Saturating concentrations (2 μg/ml) of [$^{125}$I]-281-2 in DMEM + 5% FBS were added to either the apical or basal compartments of the Transwell unit. Medium containing 10 μg/ml cold 281-2 was present on the opposite side of the filter to quench binding of any radiolabel that might diffuse across the filter. Generally, <0.7% of the label was found to diffuse from one side to the other. Binding was carried out for 1 h on ice. The filters were then washed extensively and cut out for counting in a gamma counter (1470 Wizard, Wallac, Pharmacia, Piscataway, NJ).

## RESULTS

### *Expression of Wild-Type and Mutant Mouse Syndecan-1 in MDCK Cells*

A series of syndecan-1 deletion mutants was made, designated CT22, CT9, and CT1, with 22, 9, and 1 cytoplasmic residues, respectively (Figure 1A). To investigate the polarized expression of the mutant syndecan-1 molecules in epithelia, MDCK cells were stably transfected with wild-type or mutant syndecan-1, using an expression vector containing an SRα promoter and a neomycin resistance cassette. Expressing colonies were selected after cloning by immunofluorescence microscopy.

The size of the syndecan-1 mutants in MDCK cells was examined by SDS-PAGE and Western analysis. The nonglycosylated core proteins were found to run in a ladder as shown in Figure 1B. The wild-type syndecan-1 gave a single band with an apparent molecular weight of ~56 kDa, although its calculated molecular weight is 33 kDa (Saunders *et al.*, 1989), whereas the mutants had apparent molecular weights of ~54 (CT22), 51 (CT9), and 48 kDa (CT1). Syndecan-1 molecules glycosylated with glycosaminoglycan chains run as high molecular weight smears in SDS-polyacrylamide gels and are not shown in Figure 1. The relative levels of syndecan-1 expression were compared by immunodetection of syndecan-1 in slot blots of total cell extracts normalized for cell number. Wild-type and CT22 syndecan-1 had similar levels, whereas CT9 had an approximately threefold greater level of expression (Figure 1C). Controls with untransfected MDCK cells gave totally negative results in this assay. Thus the differences described below between the wild-type and mutant syndecans cannot be explained by differences in expression levels.

### *A Deletion of the Last 12 Amino Acids in the Cytoplasmic Tail of Syndecan-1 Results in Mistargeting of the Molecule*

To determine whether wild-type and the mutant syndecan-1 molecules are expressed in a polarized fashion, cells were grown to confluency on coverslips and stained

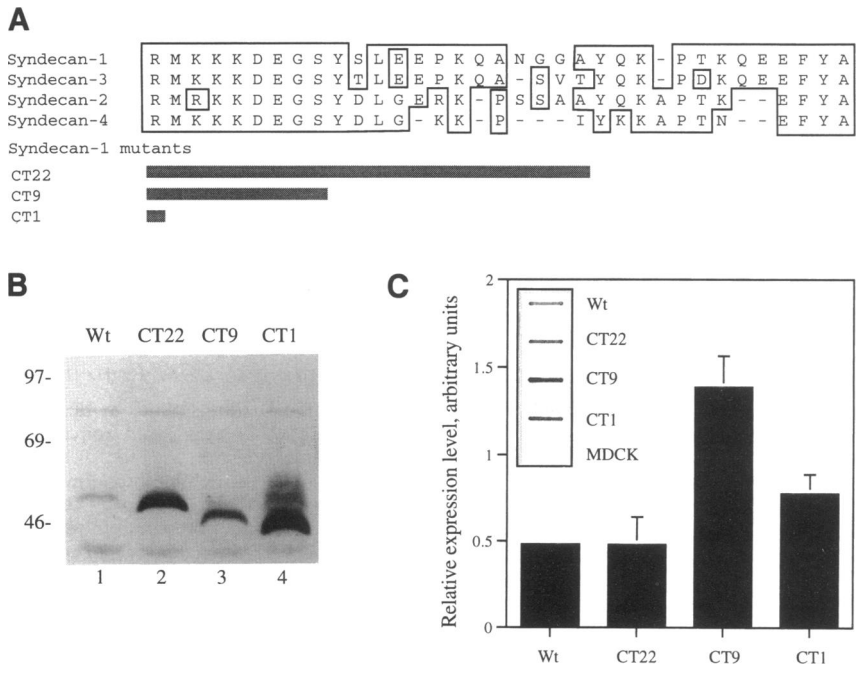


**Figure 1.** (A) Amino acid sequences for the cytoplasmic domains of the syndecan family shown in single letter amino acid code. Conserved amino acids are contained within the boxed areas. Syndecans-1 and -3, and -2 and -4 are shown next to each other based on their degree of conservation (Bernfield *et al.*, 1992). The cytoplasmic domain of syndecan-1 is 100% conserved between species. The cytoplasmic mutants generated for murine syndecan are shown below the comparative sequences; the bars represent the residues present in the mutants. The mutants were generated by oligonucleotide-directed mutagenesis as described in MATERIALS AND METHODS. (B) Western analysis of wild-type and mutant syndecan-1 core proteins in transfected MDCK cells. Monolayers were extracted with TX-100, precipitated, run on 10% SDS-PAGE, transferred onto nitrocellulose membrane, and blotted as described previously. Lane 1, MDCK wild-type syndecan-1; lane 2, MDCK CT22 mutant syndecan-1; lane 3, MDCK CT9 mutant syndecan-1; lane 4, MDCK CT1 mutant syndecan-1 (lane loading not normalized). Molecular weight markers are indicated at the left. (C) Quantitation of the relative levels of syndecan-1 expression in MDCK cell lines transfected with wild-type and mutant syndecan-1. (Insert) Total cell protein extracts were normalized for cell number, vacuum blotted onto Hybond N+, and immunodetected as described in MATERIALS AND METHODS. Quantitative analysis was carried out by image analysis. Data shows average and range of two independent experiments.

for mouse syndecan-1 either before or after fixation and permeabilization. The degree of cell polarity was examined by staining of E-cadherin (uvomorulin), a cell-cell adhesion molecule found highly concentrated in the epithelial junctional complexes and particularly in the zonula adherens (Behrens *et al.*, 1985; Boller *et al.*, 1985).

Wild-type mouse syndecan-1 was shown to be polarized to the basolateral surfaces as expected (Figure 2, A and B). Nonpermeabilized MDCK transfectants that formed a tight monolayer showed no staining with 281-2, a mAb against syndecan-1 ectodomain (Jalkanen *et al.*, 1985), indicating that all of the wild-type syndecan-1 was on the basolateral surface and thus inaccessible for binding by the antibody (Figure 2A). After permeabilization wild-type syndecan-1 became accessible to the antibody and stained the basolateral surfaces (Figure 2B). All of the syndecan-1 mutants exhibited cell surface staining before permeabilization, indicating that the protein was expressed apically (Figure 2, D, G, and J). After permeabilization the mutants were detected on both the apical and basolateral surfaces (Figure 2, E, H, and K). Staining of parallel coverslips with a mAb against E-cadherin showed that the MDCK cells expressing wild-type or any of the mutant mouse syndecans had formed a polarized monolayer (Figure 2, C, F, I, and L). These results show that the deletion of 12 or more C-terminal residues from the cytoplasmic tail

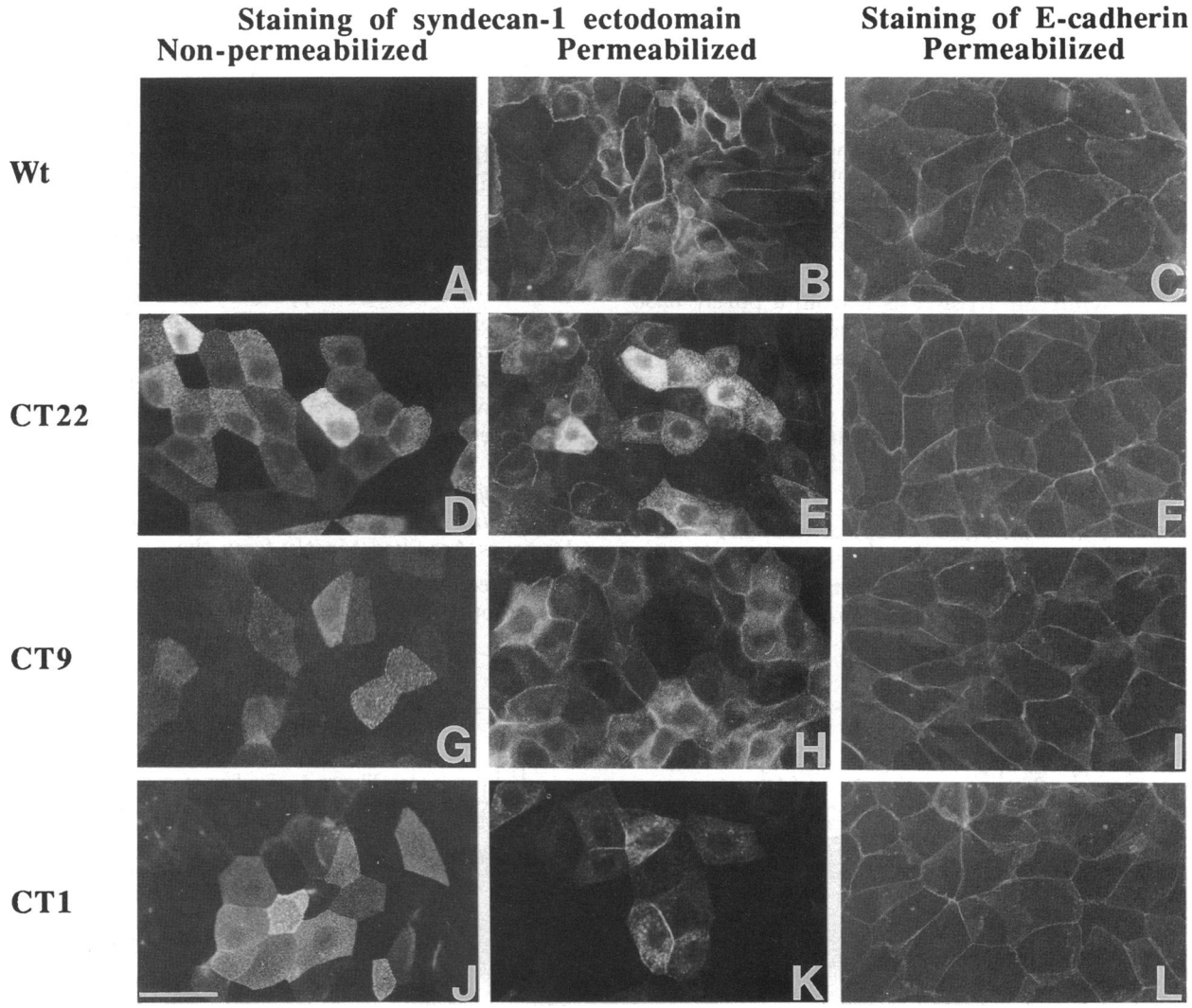


**Figure 2.** Immunofluorescence localization of wild-type and mutant syndecan-1 in stably transfected MDCK cells. MDCK cells expressing wild-type syndecan-1 (A, B, and C) or mutants CT22 (D, E, and F), CT9 (G, H, and I), or CT1 (J, K, and L) were incubated with 281-2 mAb against syndecan-1 before (A, D, G, and J) or after (B, E, H, and K) fixation and permeabilization as described in MATERIALS AND METHODS. To show that the cells were polarized, parallel coverslips were incubated after fixation and permeabilization with a mAb against canine E-cadherin (uvomorulin) (C, F, I, and L). Bar, 30 $\mu$m.

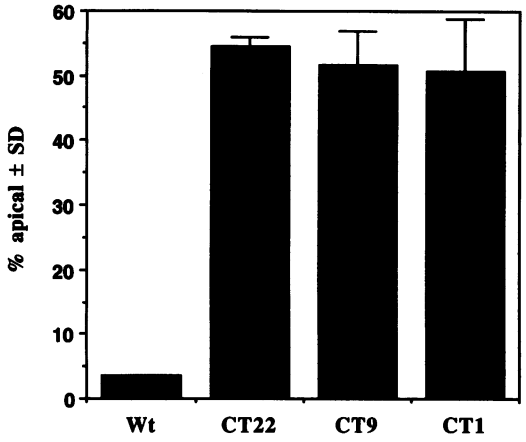


**Figure 3.** Polarized surface expression of wild-type and mutant mouse syndecan-1 molecules in transfected MDCK cells detected with [$^{125}$I]-anti-syndecan-1 mAb. Confluent monolayers were grown on polycarbonate filters. [$^{125}$I]-281-2 was added either to the apical or the basal side of the filter unit. The cells were incubated for 1 h on ice and rinsed with PBS; the filters were excised for counting in a gamma counter. The total radioactivity (100% = apical + basal) ranged from 4000 to 9000 cpm, depending on the cell line. Less than 0.7% of the total radioactivity leaked from one compartment to the other during the incubation, indicating that the cells had formed a polarized monolayer. Each bar represents the average from three experiments ±SD.

of mouse syndecan-1 converts it from a purely basolateral protein to a molecule that is expressed at both the basolateral and apical cell surfaces.

### *Syndecan-1 Mutants Are All Localized Equally at the Apical and the Basolateral Surfaces of Transfected MDCK Cells*

To quantify the distribution of apical versus basolateral syndecan-1, transfected MDCK cells grown on polycarbonate filters were incubated for 1 h on ice with iodinated anti-mouse syndecan-1 mAb added either to the apical or to the basal side. Both apical and basal media were collected to calculate leakage between the two compartments, and the filters were excised. Less than 0.7% of the label diffused across the filters during the incubation, indicating that the cells formed a tight monolayer. As shown in Figure 3, wild-type mouse syndecan-1 was expressed almost exclusively basolaterally (>96%), whereas all the mutants were expressed equally on both the apical and the basolateral side of the cells.

### *The Binding Properties of Mutant Syndecan-1 Are Not Altered*

Syndecan-1 molecules have been demonstrated to bind various ECM proteins and are thought to act as matrix receptors at the cell surface. Binding of syndecan-1 to matrix proteins at the basolateral surface might thus contribute to polarization of the molecule. We therefore investigated whether the deletion mutants exhibited any changes in their ECM-binding properties that could explain their reduced basolateral retention. Syndecan-1 derived from epithelial cells has previously been shown to bind fibrillar collagens and, less strongly, fibronectin but does not bind the major basement membrane protein laminin (Koda *et al.*, 1985; Elenius *et al.*, 1990). Solid phase-binding assays showed strong binding by all of the syndecans to type I collagen (Figure 4A) and weaker binding to fibronectin (Figure 4B). No differences in binding that could account for the observed pattern of polarization were apparent. No binding of syndecan-1 to equivalent amounts of bovine serum albumin (BSA) was detected.

### *Wild-Type Mouse Syndecan-1 Is Shed Predominantly from the Basal Side, Whereas the Mutants Are Shed Mostly from the Apical Side*

It has been previously shown that syndecan-1 is shed from mouse mammary epithelial cells by cleavage of its

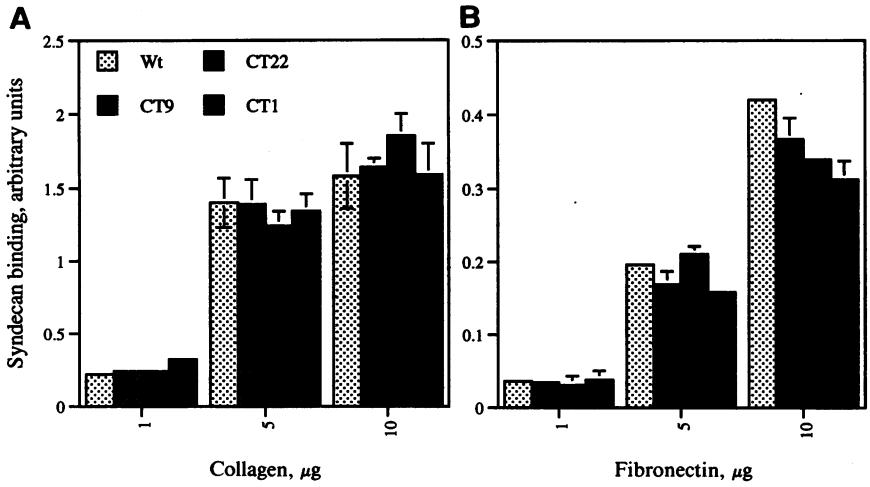


**Figure 4.** Binding of syndecan-1 to collagen and fibronectin. Collagen (type I) (A) and human plasma fibronectin (B) were diluted in PBS, and the amounts indicated on the x-axis were vacuum-blotted through slots onto nitrocellulose filters. After blocking the filters were incubated overnight at 4°C with wild-type or mutant syndecan-1, obtained by trypsin-mediated release of cell surface syndecan-1, and normalized for concentration. After washing bound syndecan-1 was immunodetected as described in MATERIALS AND METHODS. Binding was quantified by image analysis. Each bar represents the average and SD of triplicate slots within the same experiment. No binding of syndecan-1 to BSA controls was observed.

ectodomain (Jalkanen *et al.*, 1987). To examine the possibility that wild-type syndecan-1 is not detected on the apical surface of MDCK cells because of rapid cleavage of its ectodomain, cells were again grown on polycarbonate filter units. When cells had been confluent for 3–4 d, they were labeled for 7 h with $^{35}SO_4$, after which the medium was collected from the apical and basal sides and the cells were extracted with TX-100. All fractions were immunoprecipitated after preclearance with Sepharose CL-4B, using 281-2 coupled to Sepharose CL-4B, and run on a 3–15% SDS-PAGE. In addition, identically prepared samples from a separate experiment were run on a 0.7% agarose gel for more accurate quantitation. Wild-type mouse syndecan-1 was shed almost exclusively from the basal side of the MDCK cells (see Figure 5, A and B, lanes 2 and 3), whereas CT22 and CT1 mutants were predominantly shed from the apical side (see Figure 5A, lanes 8, 9, 14, and 15 and Figure 5B, lanes 8 and 9). This suggests that the steady-state distribution of the full-length mouse syndecan-1 is due to targeted transport rather than selective shedding.

The discrepancy between the amount of basolateral mutant syndecan-1 in the plasma membrane (Figure 3) and the amount of shed basolateral mutant syndecan-1 (Figure 5, A and B) is presumably due to some adherence of the ectodomain to the polycarbonate filter and/or extracellular matrix proteins. This difference, however, does not change the interpretation of the data.

### *BFA Treatment Inhibits Apical Transport of Mutant Syndecan-1 Molecules*

To further examine the sorting path used by syndecan-1 in MDCK cells, we investigated the effect of BFA on targeting. In MDCK cells basolateral sorting and basolateral to apical transcytosis routes can be distinguished based on their differential sensitivity to BFA. Treatment with BFA also disrupts apical sorting and basolateral to apical transport (Hunziker *et al.*, 1991; Low *et al.*, 1992; Matter *et al.*, 1993; Barosso and Sztul, 1994).

The transport of $^{35}SO_4$-labeled syndecan-1 was examined in the presence of 10 μg/ml BFA. BFA treatment resulted in a 70% overall reduction of total $^{35}SO_4$-labeled syndecan-1 and an apparent increase in molecular weight of the glycoslyated molecules (Figure 5A). This may be caused by an increase in the length or number of the glycosaminoglycan chains (Uhlin-Hansen and Yanagishita, 1993). Targeting of wild-type syndecan-1 was not altered by BFA (Figure 5, A and B, lanes 5 and 6), suggesting that sorting and any recycling of wild-type syndecan-1 to the basolateral surface occurs via BFA-insensitive routes. In contrast, the two mutants examined, CT22 and CT1, were mistargeted in the presence of BFA and found to be shed from the basal side in roughly equal quantities to the wild-type molecule (Figure 5A, lanes 11, 12, 17, and 18 and Figure 5B, lanes 11 and 12). BFA treatment thus blocked the apical transport of the mutant syndecan-1, as previously reported for other molecules.

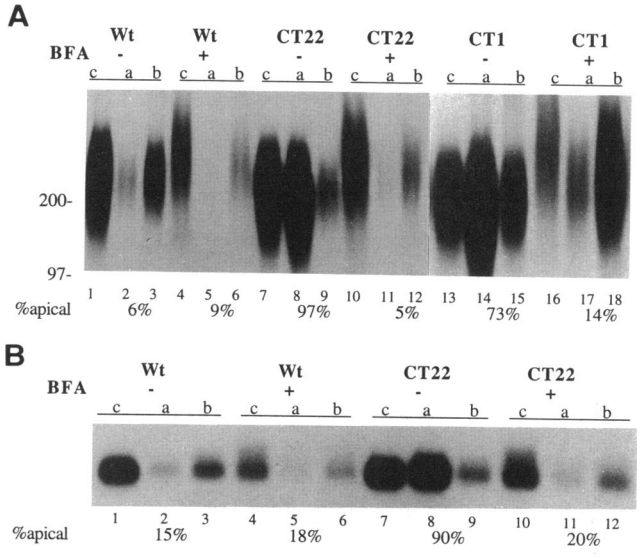


**Figure 5.** Syndecan-1 mutants are shed predominantly from the apical side of transfected MDCK cells. (A) Confluent monolayers of MDCK transfectants grown on polycarbonate filters were labeled overnight with $^{35}SO_4$. Apical and basal medium was collected, and cells were extracted with TX-100. All fractions were precleared with Sepharose CL-4B and immunoprecipitated with 281-2 coupled to Sepharose CL-4B. Samples were analyzed by 3–15% linear gradient SDS-PAGE and autoradiography. Molecular weight markers are shown on the left. Abbreviations: c, syndecan-1 extracted from cells by TX-100; a, apically shed syndecan-1; b, basally shed syndecan-1. Lanes 1–6, wild-type syndecan-1; lanes 7–12, CT22 mutant syndecan-1; lanes 13–18, CT1 mutant syndecan-1. (B) Labeling, extractions, and immunoprecipitations as above. Samples were analyzed by 0.7% agarose gel electrophoresis and autoradiography. Abbreviations as above. Lanes 1–6, wild-type syndecan-1; lanes 7–12, CT22 mutant syndecan-1. All quantitations were carried out using a microcomputer image analyzer.

### *Expression of Wild-Type and Mutant Mouse Syndecan-1 in CHO Cells*

To examine the role of the cytoplasmic domain in the transport of syndecan-1 in nonpolarized fibroblast-type cells, wild-type and mutant syndecans were inserted into an amplifiable expression vector, pFRSV, for stable expression in CHO cells. Transfected cells were selected in increasing concentrations of methotrexate (MTX) and thereafter maintained in 20 μM MTX. A heterogeneous uncloned population of cells was used in all experiments.

Western analysis of syndecan-1 expressed in CHO cells revealed two distinct bands (Figure 6A). Wild-type syndecan-1 gave a strong band at 80 kDa and a very weak band at 50 kDa. Similar double bands have previously been reported for both syndecan-1 (Carey *et al.*, 1994) and syndecan-2 (Marynen *et al.*, 1989; Cizmeci-Smith *et al.*, 1993). CT22 gave bands at ~79 and 48

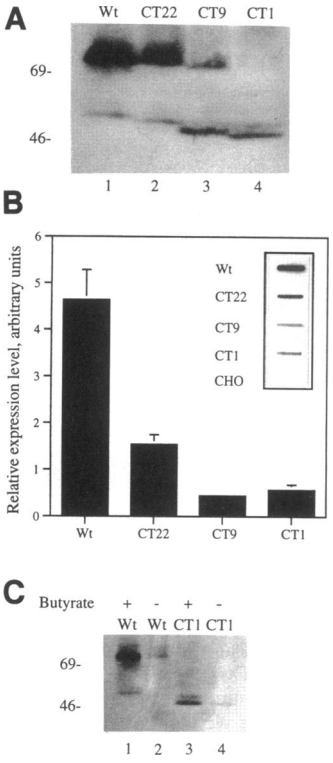


**Figure 6.** (A) Western analysis of the syndecan-1 core proteins in the CHO transfectants. Extractions, precipitations, gel electrophoresis, and Western analysis were performed as described in MATERIALS AND METHODS. Lane 1, wild-type syndecan-1; lane 2, CT22 mutant syndecan-1; lane 3, CT9 mutant syndecan-1; lane 4, CT1 mutant syndecan-1. Molecular weight markers are indicated at the left. (B) Quantitation of the relative levels of syndecan-1 expression in CHO cell lines transfected with wild-type and mutant syndecan-1. (Insert) Total cell protein extracts were normalized for cell number, vacuum blotted onto Hybond N+, and immunodetected as described in MATERIALS AND METHODS. Quantitative analysis was carried out by image analysis. Data shows average and range of two independent experiments. (C) Western analysis of wild-type and CT1 syndecan-1 core proteins expressed in CHO cells in the presence or absence of sodium butyrate. Lanes 1 and 2, cells cultured with sodium butyrate; lanes 3 and 4, cells cultured without sodium butyrate. Lanes 1 and 3, wild-type syndecan-1; lanes 2 and 4, CT1 syndecan-1. Molecular weight markers are indicated at the left.

kDa, CT9 at ~78 and 47 kDa, and CT1 only at 46 kDa. As in MDCK cells, syndecan-1 with glycosaminoglycan chains attached runs as a high molecular weight smear and is not visible in Figure 6.

Quantitation of the relative expression levels of the syndecans by protein slot blot showed that wild-type syndecan had the highest expression levels, approximately fourfold higher than those of the mutants (Figure 6B). Furthermore, when expression levels were altered by growing the cells in the presence or absence of sodium butyrate, an agent that enhances expression of certain transfected DNA constructs (Gorman *et al.*, 1983), the apparent molecular weights remained the same (Figure 6C). Therefore a higher expression level of wild-type syndecan-1 compared with CT1 does not cause the size differences seen on SDS-polyacrylamide gels. Thus the differences seen between the wild-type and mutant syndecans are not due to excessive differences in expression levels.

### *The Last 23 Amino Acids of the Mouse Syndecan-1 Cytoplasmic Tail Are Required for Efficient Exit from the ER*

To determine whether all of the mutant molecules were transported to the cell surface, the transfected CHO cells were incubated for 1 h on ice with antibody to mouse syndecan-1 ectodomain (281-2), fixed in PFA and prepared for immunofluorescence microscopy. As shown in Figure 7, all the mutants were detected at the cell surface and gave rise to staining patterns resembling that of wild-type mouse syndecan-1.

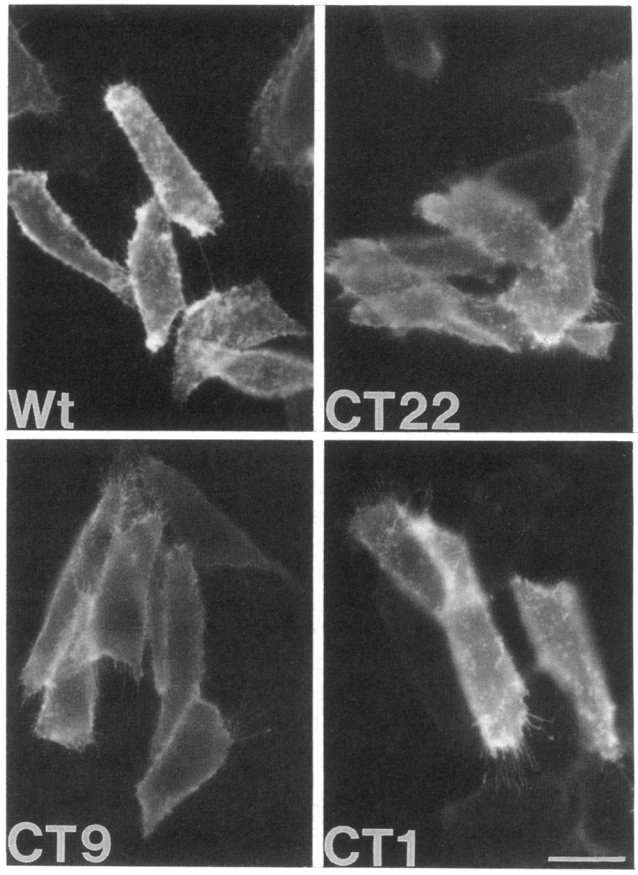


**Figure 7.** Immunofluorescence staining of wild-type and mutant mouse syndecan-1 on the plasma membrane of stably transfected CHO cells. Cells on coverslips were incubated for 1 h on ice with 50 μg/ml mAb 281-2, against mouse syndecan-1 ectodomain, rinsed with PBS, fixed with 2.5% PFA, and incubated 1 h with FITC-conjugated rabbit anti-rat IgG. Abbreviations: Wt, wild-type syndecan-1; CT22, CT9, and CT1, deletion mutants containing 22, 9, or 1 amino acids, respectively, in the cytoplasmic tail. Bar, 20 μm.

Although all of the mutant syndecans were able to reach the cell surface, intracellular staining after permeabilization with TX-100 revealed that the CT9 (Figure 8C) and CT1 (Figure 8D) deletion mutants appeared to accumulate intracellularly in a compartment resembling the ER. In contrast, the strongest sites of intracellular immunostaining for wild-type (Figure 8A) and CT22 syndecan-1 (Figure 8B) were vesicles.

To determine whether the reticular-staining pattern produced by CT9 and CT1 was caused by retention of these mutants in the ER, CHO cells expressing the wild-type syndecan-1 were incubated with BFA. In most cell lines, including CHO cells, BFA causes breakdown of the Golgi stack and the return of resident Golgi proteins to the ER (Doms *et al.*, 1989; Lippincott-Schwartz *et al.*, 1989). CHO cells expressing the wild-type mouse syndecan-1 were incubated for 5 h at 37°C with 6 μg/ml BFA, rinsed with PBS, and either fixed immediately or chased in normal medium for 30 min before fixation and staining. As shown in Figure 8E, syndecan-1 was found to accumulate in a reticular compartment with only faint staining visible elsewhere in the cell. This staining pattern was very similar to that seen in CHO cells expressing CT9 and CT1, suggesting that the retention of these mutant molecules took place in the ER. After a 30-min chase the wild-type syndecan-1 had largely moved out from the reticular compartment, presumably to the Golgi-apparatus and transport vesicles (Figure 8F). The above data suggest that the last 12 amino acids of the cytoplasmic tail are not required for normal exit from the ER, whereas a 25– or 33–amino acid deletion results in partial retention of syndecan-1 in the ER.

To investigate whether the predominantly lower molecular weight forms of the CT9 and CT1 proteins (as shown in Figure 6A) are caused by inhibition of further processing due to retention in the ER, the effect of BFA on the bands detected in Western blots was also ex-

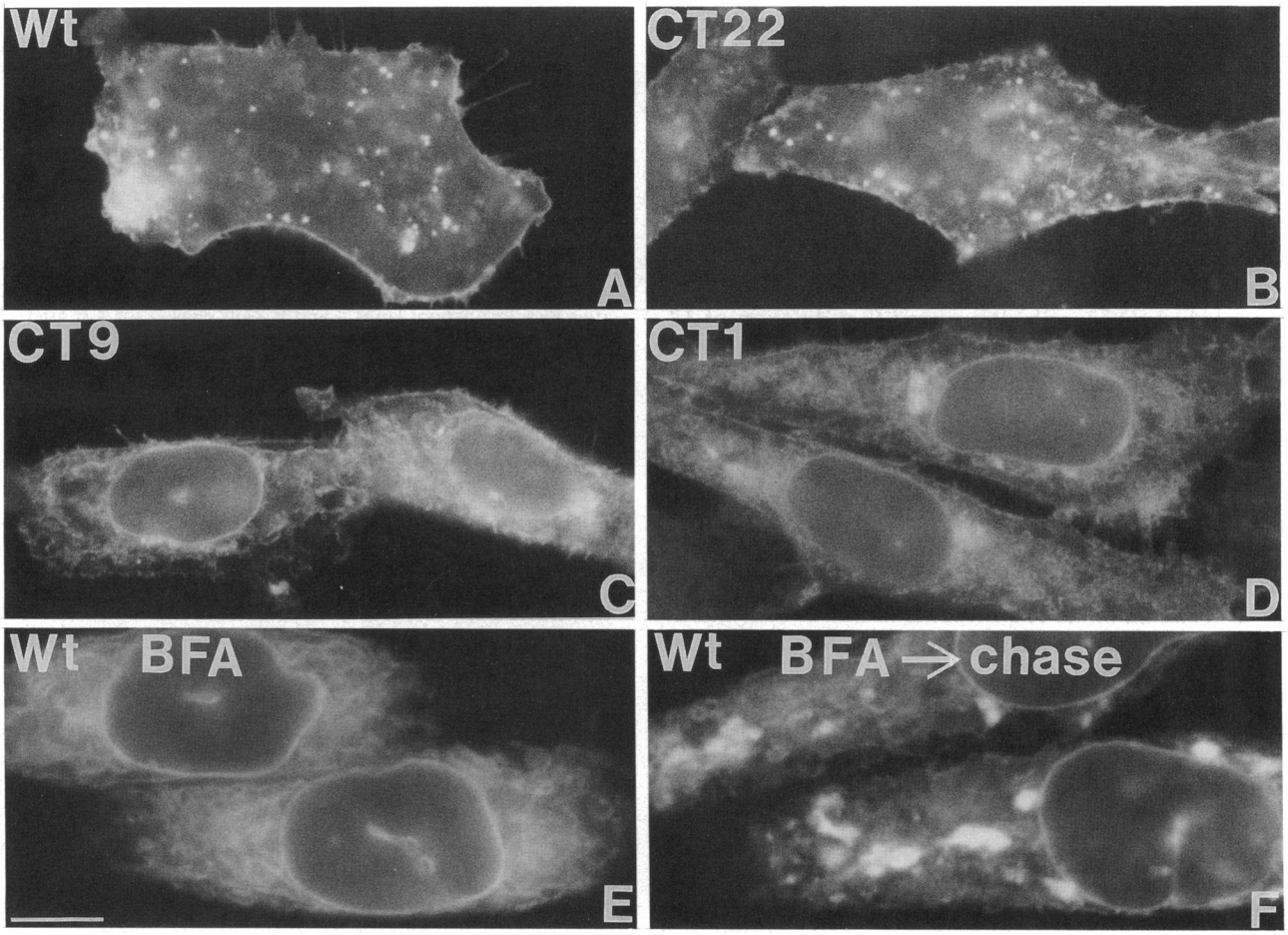


**Figure 8.** Immunofluorescence localization of wild-type and mutant mouse syndecan-1 on the plasma membrane and intracellularly in transfected CHO cells. Cells were fixed with 2.5% PFA, permeabilized with 0.5% TX-100, incubated with 50 μg/ml mouse syndecan-1 antibody, 281-2, followed by FITC-conjugated rabbit anti-rat IgG. Cells in E and F were incubated before fixation for 5 h at 37°C with 6 μg/ml BFA and chased for 0 (E) or 30 min (F). (A, E, and F) CHO cells expressing wild-type syndecan-1, (B) CHO cells expressing CT22 mutant syndecan-1, (C) CHO cells expressing CT9 mutant syndecan-1, and (D) CHO cells expressing CT1 mutant syndecan-1. Bar, 10 μm.

amined. Cells expressing wild-type or CT1 syndecan-1 were incubated for 5 h with 6 μg/ml BFA followed by a 1- or 4-h chase. As shown in Figure 9A, BFA treatment had no effect on the wild-type bands, whereas the CT1 molecule that accumulated upon treatment with BFA had a similar size (70 kDa) to the wild-type molecule (77 kDa). After a 1- or 4-h chase, newly synthesized, low molecular weight form CT1 core protein started to accumulate again (Figure 9A, lanes 7 and 8). A very faint band could also be seen at ~53 kDa in CHO cells expressing the wild-type syndecan-1 (Figure 9A, lanes 3 and 4). Addition of the protein synthesis inhibitor cycloheximide during the post-BFA chase prevented the reappearance of the low molecular weight forms of CT1 and wild-type syndecan-1 (Figure 9B, lanes 3, 4, 7, and 8). This would suggest that syndecan-1 is initially synthesized as the low molecular weight core protein and that the higher molecular weight molecule is an intermediate processing form of syndecan-1 (Carey *et al.*, 1994). Furthermore, it appears that modification by, or association with, some protein normally resident in the Golgi is required for formation of the higher molecular weight band.

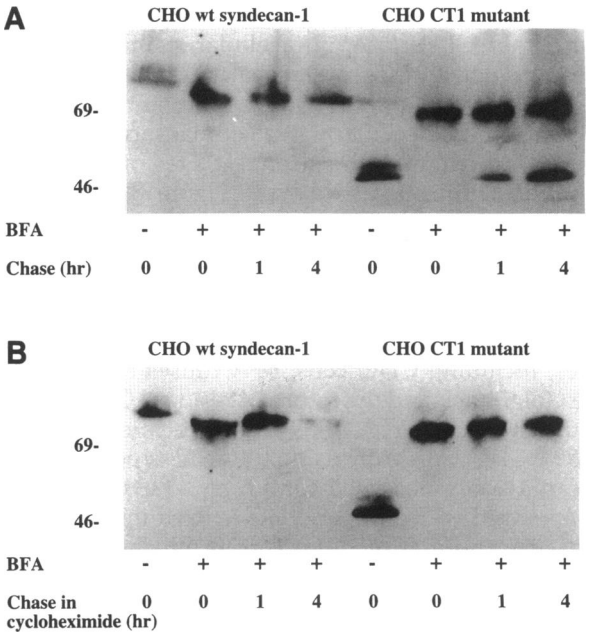


**Figure 9.** Western analysis of wild-type and CT1 mutant syndecan-1 in CHO transfectants incubated in the presence or absence of BFA. (A) Cells were incubated for 5 h in the presence or absence of 6 μg/ml BFA, as indicated in the figure. Cells were rinsed with PBS and chased in normal medium for 0, 1, or 4 h before extraction on ice. Samples were prepared as described in MATERIALS AND METHODS, separated by SDS-PAGE, and transferred to a nylon membrane; syndecan-1 was detected after incubation with 281-2 antibody by ECL. Lanes 1–4, wild-type syndecan-1; lanes 5–8, CT1 mutant. Lanes 1 and 5, cells grown in the absence of BFA; lanes 2 and 6, cells grown in the presence of BFA, no chase; lanes 3 and 7, cells chased for 1 h after BFA incubation; lanes 4 and 8, cells chased for 4 h after BFA incubation. (B) Cells were incubated as above, except that the chase was carried out in the presence of 25 μg/ml cycloheximide to prevent protein synthesis. Lanes 1–8, as above.

## DISCUSSION

### *The Membrane-Distal Part of the Syndecan-1 Cytoplasmic Tail is Required for Correct Targeting in Transfected MDCK Cells*

To examine the sorting requirements for syndecan-1, we expressed wild-type syndecan-1 and three deletion mutants in MDCK cells. We found that deletion of 12, 25, or 33 amino acids from the 34-residue cytoplasmic tail altered the steady-state localization of syndecan-1, resulting in roughly equal quantities of the proteoglycan on the apical and basolateral plasma membranes.

To exclude the possibility that the mutants are apically distributed because of decreased binding to ECM molecules, we examined the binding of the wild-type and mutant syndecan-1 to fibronectin and collagen. No clear binding differences were detected, suggesting that the apical localization of the mutants is not due to altered ECM binding on the basolateral side.

Another mechanism by which wild-type syndecan-1, but not the mutants, could be restricted to the basolateral surface is by interaction with the basolateral cytoskeleton. Studies on the $Na^+$, $K^+$-ATPase, and E-cadherin suggest that their steady-state basolateral distribution may not be the result of polarized sorting at the trans-Golgi network but is rather caused by selective retention of the molecule by the basolateral cytoskeleton (Nelson *et al.*, 1990; Hammerton *et al.*, 1991). It has previously been reported that syndecan-1 associates at the basolateral surfaces of NMuMG cells with the actin filament network (Rapraeger *et al.*, 1986). To date, however, there is no direct evidence indicating that syndecan-1 interacts with the cytoskeleton, because the insolubility of syndecan-1 in TX-100 is caused by its glycosaminoglycan chains rather than by a cytoplasmic interaction with the cytoskeleton (Miettinen and Jalkanen, 1994).

A deletion of the cytoplasmic tail of another cell-matrix adhesion molecule, CD44, results in mostly apical distribution (Neame and Isacke, 1993). Although this molecule has been shown to interact with the cytoskeleton of some cells (Tarone *et al.*, 1984; Lacy and Underhill, 1987; Camp *et al.*, 1991), no such interaction could be detected in transfected MDCK cells based on extractions with TX-100 (Neame and Isacke, 1993). The apical localization of CD44 is thus also likely to be caused by mistargeting or efficient transcytosis, rather than a lack of cytoskeletal stabilization.

Mutagenesis studies of other basolaterally sorted proteins, such as the polymeric immunoglobulin receptor (pIgR), Fc receptor (FcR), low density lipoprotein receptor (LDLR), lysosomal acid phosphatase, and vesicular stomatitis virus G protein, have not revealed any apparent common sorting determinants. Many of these

receptors, however, contain a tyrosine residue that forms part of the basolateral targeting signal. Mutagenesis studies and sequence comparison has lead to the proposal of multiple targeting signals (Table 1). When the cytoplasmic tail sequence of syndecan-1 was compared with all of the above basolateral targeting motifs, a clear correlation was noted with the targeting motif proposed by Matter *et al.* (1994). The syndecan-1 cytoplasmic tail contains amino acids $Y_{23}Q_{24}$ followed by carboxylterminal acidic residues (glutamic acids $E_{30}E_{31}$) (see Figure 1A). It is thus possible that this sequence is required for steady-state basolateral localization of syndecan-1. Further mutagenesis will be needed to confirm this hypothesis.

### *The Effects of BFA on the Steady-State Distribution of Cell Surface Membrane Proteins*

Various studies using BFA have revealed that the sorting and steady-state distribution of proteins in MDCK cells is more complex than initially anticipated. BFA was found to abolish the apical targeting of dipeptidyl peptidase IV, suggesting an effect on the formation and/or transport of apical transport vesicles (Low *et al.*, 1992). Similarly, the basolateral transport of pIgR was inhibited by BFA (Apodaca *et al.*, 1993), whereas the basolateral targeting of E-cadherin was found to be unaffected (Low *et al.*, 1992). It is thus possible that different basolateral proteins have distinct transport mechanisms that vary in their sensitivity to BFA.

The steady-state distribution of some proteins is also affected by transcytosis. Here again, the effect of BFA has been shown to vary depending on the protein examined. The basolateral to apical transcytosis of the poly-Ig receptor and a chimeric FcRII-LDLR is either inhibited or reduced by BFA (Hunziker *et al.*, 1991; Matter *et al.*, 1993). In contrast, the galactose-binding protein ricin and the fluid phase marker HRP are both transcytosed to the apical surface with increased efficiency in the presence of BFA (Prydz *et al.*, 1992).

Our data demonstrate that incubation with BFA reduced the apical distribution of the mutant syndecan-1 molecules. Because BFA treatment has been shown to prevent basolateral to apical transport of receptors in MDCK cells (Hunziker *et al.*, 1991; Matter *et al.*, 1993; Barosso and Sztul, 1994), we speculate that the basolateral confinement of the mutants in BFA-treated cells could be the result of a block in basolateral to apical transport. It is thus possible that both wild-type and the mutant syndecan-1 molecules are initially transported to the basolateral surface. After endocytosis, wild-type syndecan-1 is recycled back from the basolateral endosomes, whereas the mutants lacking a basolateral determinant are transcytosed to the apical surface (Matter *et al.*, 1993). Further experiments are required to confirm this possibility.

**Table 1.** Basolateral targeting signals in various proteins as determined by site-directed mutagenesis

| Protein | Basolateral targeting sequence | Reference |
|---|---|---|
| VSVG | **RQIYTDIE** | Thomas *et al.* (1993)<br>Thomas and Roth (1994) |
| HA Y543, F546 | SLQYRI**FI** | Brewer and Roth (1991)<br>Naim and Roth (1994) |
| pIgR | ..ARH**R**RNVD | Casanova *et al.* (1991)<br>Aroeti and Mostov (1994) |
| FcRII-B2 | TYSLLKHP | Hunziker and Fumey (1994)<br>Matter *et al.* (1994) |
| LAP | QP**P**G**Y**RHVAD | Prill *et al.* (1993) |
| LDLR: | | |
| distal | **GY**SYPSRQMVSLEDD | Matter *et al.* (1993) |
| proximal | **YQ**KTTEDE | Matter *et al.* (1994) |
| | Putative basolateral targeting signal | |
| Syndecan-1 | **YQ**KPTKQEE | This work |

The amino acids designated in bold letters have been shown to be essential for efficient basolateral targeting. The underlined amino acids are important but may not be absolutely required. Abbreviations: VSVG, vesicular stomatitis virus G protein; HA Y543, F546, a mutant influenza hemagglutinin with the indicated point mutations in the cytoplasmic domain; pIgR, polymeric immunoglobulin receptor; FcRII-B2, mouse macrophage IgG type II receptor; LAP, lysosomal acid phosphatase; LDLR, low density lipoprotein receptor.

### *Cytoplasmic Deletion Mutants of Mouse Syndecan-1 Are Partly Retained in the ER*

Our results demonstrate that the cytoplasmic tail of syndecan-1 is required for normal transport of the molecule from the ER to the plasma membrane. A 25– or 33–amino acid deletion of the 34 amino acid cytoplasmic tail results in a partial intracellular retention of the molecule. Both wild-type and mutant syndecan-1 migrated on SDS-polyacrylamide gels as two distinct molecular weight bands. Data obtained from chase experiments suggested that the retained lower molecular weight syndecan-1 represents the core protein, and the higher molecular weight form represents either a posttranslationally modified form of syndecan-1, a dimer, or a complex with some other molecule(s). In the case of CT1, the higher molecular weight molecule was only visible after BFA treatment, which results in fusion of the ER and Golgi stacks. Thus it is possible that Golgi-resident proteins are responsible for the processing of syndecan-1 into this higher molecular weight form. The higher molecular weight form is not thought to be an artifact caused by the BFA treatment, because it represents the major wild-type syndecan-1 molecule even in the absence of the drug. Furthermore, heparitinase- and chondroitinase-digested $^{35}$S-methionine labeled wild-type syndecan-1 runs on SDS-PAGE with a similar

apparent molecular weight as the higher molecular weight form detected by Western analysis (corroborative data).

All the members of the syndecan family that have been cloned so far, run on SDS-polyacrylamide gels with apparent molecular weights that are significantly larger than those predicted from their cDNA sequences, possibly because of an extended conformation caused by high proline content (see Bernfield *et al.*, 1992 for review). The higher molecular weight band reported here for CHO cells may represent an intermediate processing form, produced by posttranslational modification (Carey *et al.*, 1994), dimerization, or complexing with some other molecule. Treatment with 8 M urea, boiling under reducing conditions or in 3% SDS had no effect on the size of the syndecan-1 bands seen in CHO cells, indicating that neither disulfide nor noncovalent bonds contribute to the size of these bands (corroborative data). Syndecan-1 core protein derived from different systems has previously been reported to migrate with apparant molecular weight similar to either the smaller (53 kDa, Rapraeger *et al.*, 1985; 50 kDa, Cizmeci-Smith *et al.*, 1992) or larger (88 kDa, David *et al.*, 1992; 77 kDa, Pierce *et al.*, 1992; 80 kDa, Woods and Couchman 1994) bands reported here for wild-type syndecan-1 from CHO cells. Thus it may be that differential processing of syndecan-1 core protein, before addition of glycosaminoglycan chains, occurs in different cell types. The nature of the modification that results in the higher molecular weight form of syndecan-1 in CHO cells is currently under investigation. Whether such differential processing of the syndecan core proteins is of biological significance remains to be determined.

### *Role of the Conserved Cytoplasmic Domain*

As shown in Figure 1, the cytoplasmic domain of the syndecans are extremely conserved, in particular containing three totally conserved tyrosine residues. Proposed functions of this tail and the tyrosine residues have included cytoskeletal interactions, targeting, internalization, and shedding.

In this paper we have demonstrated that a motif contained within the final 12 amino acids of the cytoplasmic tail, possibly including one of the tyrosine residues, is required for steady-state basolateral localization of syndecan-1 in MDCK cells. We have not, however, demonstrated that this region of the tail is sufficient for basolateral targeting. This part of the tail is almost totally conserved between syndecan-1 and -3 and is highly similar between syndecan-1 and -3 and syndecan-2 and -4. Syndecan-4, however, lacks the critical glutamine residue of the proposed targeting signal (Figure 1). Targeting of syndecans-2, -3, and -4 in polarized cells has not yet been examined, however, the in vivo distribution patterns for syndecans-2 and -4 do not suggest that these molecules have a polarized distribution (for review see Elenius and Jalkanen, 1994). Syndecan-2 is expressed predominantly in mesenchymal cells and does not appear to be expressed in epithelial cell lines (Marynen *et al.*, 1989; Lories *et al.*, 1992), thus the significance of a polarization signal for its biological activity is unclear. Syndecan-4 is expressed in both fibroblasts and epithelial cell lines (David *et al.*, 1992), but no polarization has been demonstrated as yet. Syndecan-3 is expressed in nervous tissue, including neuronal cells (Carey *et al.*, 1992). As neurons can also show polarized distribution of proteins into axonal and somal domains, a potential targeting sequence may also be biologically relevant for the function of syndecan-3 (Dotti and Simmons, 1990; Dotti *et al.*, 1993).

Deletion of the last 25 amino acids of the tail was required to result in retention of syndecan-1 in the ER of CHO cells. Because CT22 was not retained, it appears that the residues in the middle and most variable section of the tail are required. No additional effect of removing the most broadly conserved region of the tail, residues 1–9, was observed. Such an effect, however, may have been masked by the effects of the CT22 and CT9 mutants.

Other possible functions of the cytoplasmic tail include interactions with cytoplasmic, or other transmembrane proteins, and regulation of shedding of the extracellular domain. Syndecan-4, but not syndecan-1, -2, or -3, has been shown to localize to focal adhesions in fibroblasts (Woods and Couchman 1994), an interaction that may be mediated by cytoplasmic motifs specific to syndecan-4. The generation of cytoplasmic mutants in other members of the syndecan family will also be required to resolve the importance of specific regions within this domain for the functions of individual syndecans.

## ACKNOWLEDGMENTS

We are grateful to Bruce Granger for the pBGS expression vector. We also thank Sirpa Leppä, Arto Määttä, and Dorothe Spillmann for helpful discussions. All the members of the Jalkanen group are acknowledged for good comradeship. This work was funded by research grants from the Finnish Academy (to H.M. and M.J.) and The Finnish Cancer Union, and a National Institutes of Health grant DE-09300-01 (to M.J.).

## REFERENCES

Apodaca, G., Aroeti, B., Tang, K., and Mostov, K.E. (1993). Brefeldin-A inhibits the delivery of the polymeric immunoglobulin receptor to the basolateral surface of MDCK cells. J. Biol. Chem. *268*, 20380–20385.

Aroeti, B., and Mostov, K.E. (1994). Polarized sorting of the polymeric immunoglobulin receptor in the exocytosis and endocytosis pathways is controlled by the same amino acids. EMBO J. *13*, 2297–2304.

Barosso, M., and Sztul, E.S. (1994). Basolateral to apical transcytosis in polarized cells is indirect and involves BFA and trimeric G protein sensitive passage through the apical endosome. J. Cell Biol. *124*, 83–100.

Behrens, J., Birchmeier, W., Goodman, S.L., and Imhof, B.A. (1985). Dissociation of Madin-Darby canine kidney epithelial cells by the monoclonal antibody anti-arc-1: mechanistic aspects and identification of the antigen as a component related to uvomorulin. J. Cell Biol. *101*, 1307–1315.

Bernfield, M., Kokenyesi, R., Kato, M., Hinkes, M.T., Spring, J., Gallo, R.L., and Lose, E.J. (1992). Biology of the syndecans. Annu. Rev. Cell Biol. *8*, 365–393.

Brewer, C.B., and Roth, M.G. (1991). A single amino acid change in the cytoplasmic domain alters the polarized delivery of influenza virus hemagglutinin. J. Cell Biol. *114*, 413–421.

Boller, K., Vestweber, D., and Kemler, R. (1985). Cell-adhesion molecule uvomorulin is localized in the intermediate junctions of adult intestinal epithelial cells. J. Cell Biol. *100*, 327–332.

Camp, R.L., Kraus, T.A., and Pure, E. (1991). Variations in the cytoskeletal interaction and posttranslational modification of the CD44 homing receptor in macrophages. J. Cell Biol. *115*, 1283–1292.

Carey, D.J., Evans, D.M., Stahl, R.C., Asundi, V.K., Conner, K.J., Garbes, P., and Cizmeci-Smith, G. (1992). Molecular cloning and characterization of N-syndecan, a novel transmembrane heparan sulfate proteoglycan. J. Cell Biol. *117*, 191–201.

Carey, D.J., Stahl, R.C., Cizmeci-Smith, G., and Asundi, V.K. (1994). Syndecan-1 expressed in schwann cells causes morphological transformation and cytoskeletal reorganization and associates with actin during spreading. J. Cell Biol. *124*, 161–170.

Casanova, J.E., Apodaca, G., and Mostov, K.E. (1991). An autonomous signal for basolateral sorting in the cytoplasmic domain of the polymeric immunoglobulin receptor. Cell *66*, 65–75.

Cizmeci-Smith, G., Asundi, V., Stahl, R.C., Teichman, L.J., Chernousov, M., Cowan K., and Carey, D.J. (1992). Regulated expression of syndecan in vascular smooth muscle cells and cloning of rat syndecan core protein cDNA. J. Biol. Chem. *267*, 15729–15736.

Cizmeci-Smith, G., Stahl, R.C., Showalter, L.J., and Carey D.J. (1993). Differential expression of transmembrane proteoglycans in vascular smooth muscle cells. J. Biol. Chem. *268*, 18740–18747.

David, G., van der Schueren, B., Marynen, P., Cassiman, J.-J., and van den Berghe, H. (1992). Molecular cloning of amphiglycan, a novel integral membrane heparan sulfate proteoglycan expressed by epithelial and fibroblastic cells. J. Cell Biol. *118*, 961–969.

Doms, R.W., Russ, G., and Yewdell, J.W. (1989). Brefeldin A redistributes resident and itinerant Golgi proteins to the endoplasmic reticulum. J. Cell Biol. *109*, 61–72.

Dotti, C.G., and Simons, K. (1990). Polarized sorting of viral glycoproteins to the axon and dendrites of hippocampal neurons in culture. Cell *62*, 63–72.

Dotti, C.G., Kartenbeck, J., and Simons, K. (1993). Polarized distribution of the viral glycoproteins of vesicular stomatitis, fowl plaque and Semliki Forest viruses in hippocampal neurons in culture: a light and electron microscopy study. Brain Res. *610*, 141–147.

Elenius, K., and Jalkanen, M. (1994). Function of the syndecans—a family of cell surface proteoglycans. J. Cell Sci. *107*, (*in press*).

Elenius, K., Salmivirta, M., Inki, P., Mali M., and Jalkanen, M. (1990). Binding of human syndecan to extracellular matrix proteins. J. Biol. Chem. *265*, 17837–17843.

Felgner, P.L., Gadek, T.R., Holm, M., Roman, R., Chan, H.W., Wenz, M., Northrop, J.P., Ringold, G.M., and Danielsa, G.A. (1987). Lipofection: a highly efficient, lipid-mediated DNA-transfection procedure. Proc. Natl. Acad. Sci. USA *84*, 7413–7417.

Gorman, C.M., Howard, B.H., and Reeves, R. (1983). Expression of recombinant plasmids in mammalian cells is enhanced by sodium butyrate. Nucleic Acids Res. *11*, 7631–7648.

Hammerton, R.W., Krzeminski, K.A., Mays, R.W., Ryan, T.A., Wollner, D.A., and Nelson, W.J. (1991). Mechanism for regulating cell surface distribution of $Na^+$, $K^+$-ATPase in polarized epithelial cells. Science *254*, 847–850.

Hayashi, K., Hayashi, M., Jalkanen, M., Firestone, J., Trelstad, R.L., and Bernfield, M. (1987). Immunocytochemistry of cell surface proteoglycan in mouse tissues. A light electron microscopic study. J. Histochem. Cytochem. *35*, 1079–1088.

Heinegård, D., Sommarin, Y., Hedbom, E., Wieslander, J., and Larsson, B. (1985). Assay of proteoglycan populations using agarose-polyacrylamide gel electrophoresis. Anal. Biochem. *151*, 41–48.

Horwich, A.L., Fenton, W.A., Firgaira, F.A., Fox, F.E., Kolansky, D., Mellman, I.S., and Rosenberg, L.E. (1985). Expression of amplified DNA sequences for ornithine transcarbamylase in HeLa cells: arginine residues may be required for mitochondrial import of enzyme precursor. J. Cell Biol. *100*, 1515–1521.

Hunziker, W., and Fumey, C. (1994). A di-leucine motif mediates endocytosis and basolateral sorting of macrophage IgG Fc receptors in MDCK cells. EMBO J. *13*, 2963–2969.

Hunziker, W., Whitney, J.A., and Mellman, I. (1991). Selective inhibition of transcytosis by brefeldin A in MDCK cells. Cell *67*, 617–627.

Jalkanen, M., Elenius, K., and Rapraeger, A. (1993). Syndecan: regulator of cell morphology and growth factor action at the cell-matrix interface. Trends Glycosci. Glycotech. *5*, 107–120.

Jalkanen, M., Nguyen, H., Rapraeger, A., Kurn, N., and Bernfield, M. (1985). Heparan sulfate proteoglycans from mouse mammary epithelial cells: localization on the cell surface with a monoclonal antibody. J. Cell Biol. *101*, 976–984.

Jalkanen, M., Rapraeger, A., Saunders, S., and Bernfield, M. (1987). Cell surface proteoglycan of mouse mammary epithelial cells is shed by cleavage of its matrix-binding ectodomain from its membrane-associated domain. J. Cell Biol. *105*, 3087–3096.

Kiefer, M.C., Stephans, J.C., Crawford, K., Okino, K., and Barr, P.J. (1990). Ligand-affinity cloning and structure of a cell surface heparan sulfate proteoglycan that binds basic fibroblast growth factor. Proc. Natl. Acad. Sci. USA *87*, 6985–6989.

Koda, J.E., Rapraeger, A., and Bernfield, M. (1985). Heparan sulfate proteoglycans from mouse mammary epithelial cells. Cell surface proteoglycan as a receptor for interstitial collagens. J. Biol. Chem. *260*, 8157–8162.

Kunkel, T.A., Roberts, J.D., and Zakour, R.A. (1987). Rapid and efficient site-specific mutagenesis without phenotypic selection. Methods Enzymol. *154*, 367–382.

Lacy, B.E., and Underhill, C.B. (1987). The hyaluronate receptor is associated with actin filaments. J. Cell Biol. *105*, 1395–1404.

Lippincott-Schwartz, J., Yuan, L., Tipper, C., Amherdt, M., Orci, L., and Klausner, R.D. (1991). Brefeldin A's effect on endosomes, lysosomes, and the TGN suggests a general mechanism for regulating organelle structure and membrane traffic. Cell *67*, 601–616.

Lippincott-Schwartz, J., Yuan, L.C., Bonifacino, J.S., and Klausner, R.D. (1989). Rapid redistribution of Golgi proteins into the ER in cells treated with brefeldin A: evidence for membrane cycling from Golgi to ER. Cell *56*, 801–813.

Lories, V., Cassiman, J.J., Van der Berghe, H., and David, G. (1992). Differential expression of cell surface heparan sulfate proteoglycans in human mammary epithelial cells and lung fibroblasts. J. Biol. Chem. *267*, 1116–1122.

Low, S.H., Tang, B.T., Wong, S.H., and Hong, W. (1992). Selective inhibition of protein targeting to the apical domain of MDCK cells by brefeldin A. J. Cell Biol. *118*, 51–62.

Marynen, P., Zhang, J., Cassiman, J.-J., van den Berghe, H., and David, G. (1989). Partial primary structure of the 48- and 90-kilodalton core

proteins of cell surface-associated heparan sulfate proteoglycans of lung fibroblasts. J. Biol. Chem. *264*, 7017–7024.

Matter, K., and Mellman, I. (1994). Mechanisms of cell polarity: sorting and transport in epithelial cells. Curr. Opin. Cell Biol. *6*, 545–554.

Matter, K., Yamamoto, E.M., and Mellman, I. (1994). Structural requirements and sequence motifs for polarized sorting and endocytosis of LDL and Fc receptors in MDCK cells. J. Cell Biol. *126*, 991–1004.

Matter, K., Whitney, J.A., Yamamoto, E.M., and Mellman, I. (1993). Common signals control low density lipoprotein receptor sorting in endosomes and the Golgi complex of MDCK cells. Cell *74*, 1053–1064.

Miettinen, H.M., and Jalkanen, M. (1994). The cytoplasmic domain of syndecan-1 is not required for association with Triton X-100-insoluble material. J. Cell Sci. *107*, 1571–1581.

Miettinen, H.M., Matter, K., Hunziker, W., Rose, J.K., and Mellman, I. (1992). Fc receptor endocytosis is controlled by a cytoplasmic domain determinant that actively prevents coated pit localization. J. Cell Biol. *116*, 875–888.

Miettinen, H.M., Rose, J.K., and Mellman, I. (1989). Fc receptor isoforms exhibit distinct abilities for coated pit localization as a result of cytoplasmic domain heterogeneity. Cell *58*, 317–327.

Misumi, Y., Miki, K., Takatsuki, A., Tamura, G., and Ikehara, Y. (1986). Novel blockade by Brefeldin A of intracellular transport of secretory proteins in cultured rat hepatocytes. J. Biol. Chem. *261*, 11398–11403.

Mostov, K., Apodaca, G., Aroeti, B., and Okamoto, C. (1992). Plasma membrane protein sorting in polarized epithelial cells. J. Cell Biol. *116*, 577–583.

Naim, H.Y., and Roth, M.G. (1994). Characteristics of the internalization signal in the Y453 influenza virus hemagglutinin suggest a model for recognition of internalization signals containing tyrosine. J. Biol. Chem. *269*, 3928–3933.

Neame, S.J., and Isacke, C.M. (1993). The cytoplasmic tail of CD44 is required for basolateral localization in epithelial MDCK cells but does not mediate association with the detergent-insoluble cytoskeleton of fibroblasts. J. Cell Biol. *121*, 1299–1310.

Nelson, W.J., Shore, E.M., Wang, A.Z., and Hammerton, R.W. (1990). Identification of a membrane-cytoskeletal complex containing the cell adhesion molecule uvomorulin (E-cadherin), ankyrin, and fodrin in MDCK epithelial cells. J. Cell Biol. *110*, 349–357.

Pierce, A., Lyon, M., Hampson, I.N., Cowling, G.J., and Gallagher, J.T. (1992). Molecular cloning of the major cell surface heparan sulfate proteoglycan from rat liver. J. Biol. Chem. *267*, 3894–3900.

Prill, V., Lehmann, L., von Figura, K., and Peters, K. (1993). The cytoplasmic tail of lysosomal acid phosphatase contains overlapping but distinct signals for basolateral sorting and rapid internalization in polarized MDCK cells. EMBO J. *12*, 2181–2193.

Prydz, K., Hansen, S.H., Sandvig, K., and van Deuers, B. (1992). Effects of brefeldin A on endocytosis, transcytosis and transport to the Golgi complex in polarized MDCK cells. J. Cell Biol. *119*, 259–272.

Rapraeger, A.C. (1993). The coordinated regulation of heparan sulfate, syndecans and cell behavior. Curr. Opin. Cell Biol. *5*, 844–853.

Rapraeger, A., Jalkanen, M., Endo, E., Koda, J., and Bernfield, M. (1985). The cell surface proteoglycan from mouse mammary epithelial cells bears chondroitin sulfate and heparan sulfate glycosaminoglycans. J. Biol. Chem. *260*, 11046–11052.

Rapraeger, A., Jalkanen, M., and Bernfield, M. (1986). Cell surface proteoglycan associates with the cytoskeleton at the basolateral cell surface of mouse mammary epithelial cells. J. Cell Biol. *103*, 2683–2696.

Rapraeger, A.C., Krufka, A., and Olwin, B.B. (1991). Requirement of heparan sulfate for bFGF-mediated fibroblast growth and myoblast differentiation. Science *252*, 1705–1708.

Rose, J.K., and Bergman, J.E. (1983). Altered cytoplasmic domain affect intracellular transport of the vesicular stomatitis virus glycoprotein. Cell *34*, 513–524.

Rose, J.K., Buonocore, L., and Whitt, M. (1991). A new cationic liposome reagent mediating nearly quantitative transfection of animal cells. Biotechniques *10*, 520–525.

Salmivirta, M., Elenius, K., Vainio, S., Hofer, U., Chiquet-Ehrismann, R., Thesleff, I., and Jalkanen, M. (1991). Syndecan from embryonic tooth mesenchyme binds tenascin. J. Biol. Chem. *266*, 7733–7739.

Sandvig, K., Prydz, K., Hansen, S.H., and van Deuers, B. (1991). Ricin transport in brefeldin A-treated cells: correlation between Golgi structure and toxic effect. J. Cell Biol. *115*, 971–981.

Sanger, F., Nicklen, S., and Coulson, S.R. (1977). DNA sequencing with chain-terminating inhibitors. Proc. Natl. Acad. Sci. USA *74*, 5463–5471.

Saunders, S., and Bernfield, M. (1988). Cell surface proteoglycan binds mouse mammary epithelial cells to fibronectin and behaves as a receptor for interstitial matrix. J. Cell Biol. *106*, 423–430.

Saunders, S., Jalkanen, M., O'Farrel, S., and Bernfield, M. (1989). Molecular cloning of syndecan, an integral membrane proteoglycan. J. Cell Biol. *108*, 1547–1556.

Simonsen, C.C., and Levinson, A.D. (1983). Isolation and expression of an altered mouse dihydrofolate reductase cDNA. Proc. Natl. Acad. Sci. USA *80*, 2495–2499.

Sun, X., Mosher, D.F., and Rapraeger, A. (1989). Heparan sulfate-mediated binding of epithelial cell surface proteoglycan to thrombospondin. J. Biol. Chem. *264*, 2885–2889.

Takebe, Y., Seiki, M., Fujisawa, J.-I., Hoy, P., Yokota, K., Arai, K.-I., Yoshida, M., and Arai, N. (1988). SR$\alpha$ promoter: an efficient and versatile mammalian cDNA expression system composed of the Simian virus 40 early promoter and the R-U5 segment of human T-cell leukemia virus type 1 long terminal repeat. Mol. Cell. Biol. *8*, 466–472.

Tarone, G., Ferracini, R., Galetto, G., and Comoglia, P. (1984). A cell surface integral membrane glycoprotein of 85,000 mol wt (gp85) associated with Triton X-100-insoluble cell skeleton. J. Cell Biol. *99*, 512–519.

Thornton, D.J., Nieduszynski, I.A., Oates, K., and Sheehan, J.K. (1986). Electron-microscopic and electrophoretic studies of bovine femoral-head cartilage proteoglycan fractions. Biochem. J. *240*, 41–48.

Thomas, D.C., and Roth, M.G. (1994). The basolateral targeting signal in the cytoplasmic domain of glycoprotein G from vesicular stomatitis virus resembles a variety of intracellular targeting motifs related by primary sequence but having diverse targeting activities. J. Biol. Chem. *269*, 15732–15739.

Thomas, D.C., Brewer, C.B., and Roth, M.G. (1993). Vesicular stomatitis virus glycoprotein contains a dominant cytoplasmic basolateral sorting signal critically dependent upon a tyrosine. J. Biol. Chem. *268*, 3313–3320.

Uhlin-Hansen, L., and Yanagishita, M. (1993). Differential effect of brefeldin A on the biosynthesis of heparan sulfate and chondroitin/dermatan sulfate proteoglycans in rat ovarian granulosa cells in culture. J. Biol. Chem. *268*, 17370–17376.

Wagner, M., Rajasekan, A.K., Hanzel, D.K., Mayor, S., and Rodriguez-Boulan, E. (1994). Brefeldin A causes structural and functional alterations of the trans-Golgi network of MDCK cells. J. Cell Sci. *107*, 933–943.

Wills, J.W., Srinivas, R.V., and Hunter, E. (1984). Mutations of the Rous sarcoma virus env gene that affect the transport and subcellular location of the glycoprotein products. J. Cell Biol. *99*, 2011–2023.

Woods, A., and Couchman, J.R. (1994). Syndecan-4 heparan sulfate proteoglycan is a selectively enriched and widespread focal adhesion component. Mol. Biol. Cell *5*, 183–192.

Yayon, A., Klagsbrun, J.D., Esko, J.D., Leder, P., and Ornitz, D.M. (1991). Cell surface, heparin-like molecules are required for binding of basic fibroblast growth factor to its high affinity receptor. Cell *64*, 841–848.

Zoller, M.J., and Smith, M. (1982). Oligonucleotide-directed mutagenesis using M13-derived vectors: an efficient and general procedure for the production of point mutations in any fragment. Nucleic Acids Res. *10*, 6487–6500.

Zuniga, M.C., and Hood, L.E. (1986). Clonal variation in cell surface display of an H-2 protein lacking a cytoplasmic tail. J. Cell Biol. *102*, 1–10.